

b) *Using NMP as Solvent (with p-toluenesulfonic acid)*

Conditions:

638 mmol NMP,
30.6 mmol p-toluenesulfonic acid
0.7 mmol ketene/minute
1.0 mmol acetaldehyde/minute
9.2 mmol N₂/minute
150°C
Run 5-6 hours per day for 1 to 5 days

VAM yield from ketene:

1st day = 59%
2nd day = 76%
3rd day = 77%
4th day = 71%
5th day = 68%

Accountability for the whole run:

ketene = 103%
acetaldehyde = 90%.

Can account for 75.5 g of the 80.8 g heel (diff 5.3 g).
Heel contained 1 wt % EDA.

c) *Using NMP/Ac₂O as Solvent (with p-toluenesulfonic acid)*

Conditions:

436 mol NMP
254 mmol Ac₂O
30.6 mmol p-toluenesulfonic acid
0.7 mmol ketene/minute
1.0 mmol acetaldehyde/minute
9.2 mmol N₂/minute
150°C
Run 5-6 hours per day for 1 to 5 days

VAM yield from ketene:

1st day = 59%
2nd day = 90%
3rd day = 88%

Accountability for the whole run:

ketene = 105%
acetaldehyde = 105%

Can account for 81.9 g of the 85.3 g heel (diff. 3.4 g).
Heel contained 8.3 wt % EDA.

2. *Other Catalyst Systems (with gas stripped operation):*

All use the following conditions:

30.6 mmol acid catalyst
61.6 mmol acetic acid
583 mmol acetic anhydride
0.7 mmol ketene/minute
1.0 mmol acetaldehyde/minute
9.2 mmol N₂/minute
150°C
Run 5-6 hours per day for 1 to 5 days

a) *Sulfuric acid catalyst (1 day):*

VAM yield from ketene = 41 %
Extensive coking, reactor plugged.

b) *Phosphoric acid catalyst (2 days):*

Best VAM yield from ketene = 30 %
Extensive coking, reactor plugged.

c) *Methanesulfonic acid catalyst (3 days):*

Best VAM yield from ketene = 32 %
Low tar, low activity.

d) *Boric acid catalyst (1 day):*

VAM yield from ketene = 2 %
Low activity, but heel contained 18 wt % EDA.

e) *Zeolite HY catalyst (calcined, 15.7g, no HOAc used, 1 day):*

VAM yield from ketene = 4 %
Low activity.

B. Plugged Flow Reactor with Reflux and Heterogeneous Catalyst

Conditions:

Catalyst = 17 ml (10.26 g) Amberlyst 15 (ca. 30.6 meq -SO₃H),
diluted with 15 ml 16X24 mesh quartz chips.
0.7 mmol ketene/minute
1.0 mmol acetaldehyde/minute
9.2 mmol N₂/minute
98°C (steam-heated reactor)
Run 5-6 hours per day for 5 days

Results:

VAM yield from ketene:

1st day = 10%
2nd day = 44%
3rd day = 37%
4th day = 34 %
5th day = 31%

Accountability for the whole run:

ketene = 111%
acetaldehyde = 78%

Recovered from non-volatiles trap:

8.1 g containing
39.9 wt % EDA,
2.0 wt % Ac₂O,
1.2 wt % HOAc
3.5 wt % HAc.

Eastman will continue to optimize this process using the gas-stripped reactor, but has also begun to examine alternative reactor designs under scaled-up conditions. To date, Eastman has only tested several polymeric sulfonic acid resins in a heterogeneous variation using this unit. These catalysts were inferior to the soluble arylsulfonic acids since the arylsulfonic acid resins were unable to tolerate the reaction conditions without significant degradation. Eastman will continue to examine alternative reactor designs over the next quarter using this scaled-up reactor.

Task 3.1.a. Preliminary Economics for a Ketene Based Process. Having identified operable processes at the bench scale for both the hydrogenation of ketene and the direct esterification of acetaldehyde with ketene, Eastman now has sufficient information to undertake *preliminary* economic estimates for the overall process. The conceptual flowsheet is in place. Eastman already has estimates for an appropriately sized acetic acid plant and ketene furnace, although the models will require some updating. Further, designs for the conversion of acetaldehyde and ketene to VAM are well underway. Preliminary estimates will *not* account for the available synergies between the components of the facility and will purposely be conservative.

Task 3.2. Assessment of Reductive Carbonylation. Eastman has also begun to look at what information will be needed for a direct comparison of ketene hydrogenation vs. reductive carbonylation of methanol as a source of acetaldehyde and has concluded that the literature does not contain all the pertinent information, particularly with respect to kinetics and gas pressures, required for an adequate economic estimate. Given that the hydrogenation of ketene may require an expensive cryogenic separation and that Eastman can already eliminate the acetic recycle loops through the direct esterification of acetaldehyde with ketene, this may be a critical point in discovering the best possible process. Therefore, Eastman is proposing to undertake some related investigations into the reductive carbonylation of methanol to clarify the key variables

and examine some potentially new technologies before undertaking this estimate. (This is consistent with the original proposal.)

C. Future Directions

Task 1.1. Hydrogenation of Ketene. Over the next quarter Eastman will be:

- a) pursuing a detailed study of the Pd catalysts.
- b) examining potential CO-tolerant catalysts, including homogeneous catalysts and reactor designs for this hydrogenation.

Task 2.1. Conversion of Acetaldehyde and Ketene to VAM. Over the next quarter, Eastman expects to continue its investigation of gas-stripped reactors and examine alternative designs for conducting these reactions.

Task 3.1.a. Preliminary Economics. Eastman expects to have a *preliminary* estimate completed by the end of the next quarter.

Task 3.2. Economic Comparison to Reductive Carbonylation. As discussed above, the technology descriptions given in the prior art are insufficiently detailed for an estimate, and Eastman has some new concepts that may make this the preferred acetaldehyde source. Therefore, Eastman will dedicate some of its effort to measuring the key variables in the best processes from the prior art and testing some novel concepts for the reductive carbonylation of methanol to acetaldehyde.

D. Summary

Over the last quarter, Eastman has extended its knowledge related to the hydrogenation of ketene to acetaldehyde and has identified a key knowledge gap related to poisoning by carbon monoxide. Eastman has also begun the long process of optimizing the direct esterification of acetaldehyde with ketene to produce VAM. These form a very simple overall process for the generation of VAM. Eastman will further optimize these processes over the next several months and will be generating initial cost estimates for the production of VAM from syngas by this method. This now provides two alternative methods of consuming acetic acid in the production of VAM and eliminates the large recycle loops.

Task 3.3 New Processes for Alcohols and Oxygenated Fuel Additives

3.3.1 Isobutanol Synthesis in a Three Phase System--Institute for Technical Chemistry and Petroleum Chemistry (RWTH Aachen-Germany)

Catalyst Preparation

A first goal to improve the Zr/Zn/Mn system has been to determine the influence of different synthesis methods. Coprecipitation, complexation and sol-gel methods were chosen for this purpose. In the last quarter, the focus was primarily on complexation catalysts. In this quarter, we concentrated on sol-gel methods. In addition the influence of alkali promoters was evaluated. Furthermore new catalyst systems have been tested and will be reported here. Future work

includes determination of the optimum composition and the role of additional transition and rare earth metal promoters.

Sol-Gel Catalysts

One of the methods chosen to determine the influence of preparation is sol-gel synthesis. This method involves the formation of an oxide network via zirconium alkoxides into which the other components are incorporated. In previous quarterly reports (July-Sept., Oct.-Dec. 1995) the influence of modifying agents and acids on gel formation was reported. In this report, surface characteristics and catalysis behavior are presented.

In Table 3.3.1 the BET surface areas and pore size diameters of differently prepared gels are shown. It can be seen that a supercritical drying step seems to be necessary for the development of a large surface area. A normal air drying procedure (NL72) leads to a small surface area. The use of acetic acid, which can alter gel formation by complexing to the zirconium metal or by changing pH, leads to a maximum surface area. Changing the anions of the simultaneously added zinc and manganese salts has only a slight influence on pore size and surface area. Nitric acid and acetylacetone modification leads to broader pore size distributions and smaller surface areas. From these data it can be concluded that this method provides a way to generate catalysts with specifically defined surface areas and pore size distributions over a large range.

XRD data showed that supercritical extraction leads in part to the development of crystalline zinc oxide species. Zirconium and manganese oxide seem not be affected by this treatment, showing only poor crystallization. The effect of this phenomenon on catalyst stability is currently being investigated.

Table 3.3.1 Effect on Pore Size and Surface Area by Variation of Sol-Gel Parameters

	Metal Salt	Modifying Agent ^b	Surface Area ^c in [m ² .g ⁻¹]	Mean Pore Size ^d in [Å]
NL72 ^a	nitrate	HOAc	17	40 (35-45)
NL73	nitrate	HOAc	113	55 (30-80)
NL82	acetate	HOAc	122	40 (30-50)
NL84	nitrate	HNO ₃	80	90 (50-130)
NL90	nitrate	HNO ₃ / acac	41	210 (50-330)

^a Air dried instead of supercritically dried.

^b HOAc: acetic acid; HNO₃: nitric acid; acac: acetylacetone.

^c Measured after calcination in air at 400°C.

^d Range is given in parentheses

The unpromoted sol gel materials were tested in a syngas reaction. Table 3.3.2 shows the catalysis results. The air-dried catalyst (NL72) showed only poor activity and high methane production. In contrast, the acetic acid-modified gels showed the highest activity (NL73) and selectivity (NL82) towards isobutanol, with concomitant low methane production. Again the importance of the supercritical drying step becomes evident. Acetylacetone modification led to

decreased activity. In general it can be concluded that a large surface area leads to higher productivity, as expected

Table 3.3.2 Catalysis Behavior on Variation Sol Gel Parameters^a

Cat. Zr/Zn/Mn-	NL72	NL73	NL82	NL84	NL90
STY ^b MeOH	134	968	574	601	544
STY iBuOH	23	135	159	143	102
STY Alcohols (Rest)	13	22	32	27	18
STY Methane	890	27	67	127	123
STY Alcohols	160	1125	765	771	664
STY Total Liquid	223	1371	990	989	817
Selectivity CO ₂	49	35	42	40	40
Conversion CO	55	24	26	25	23

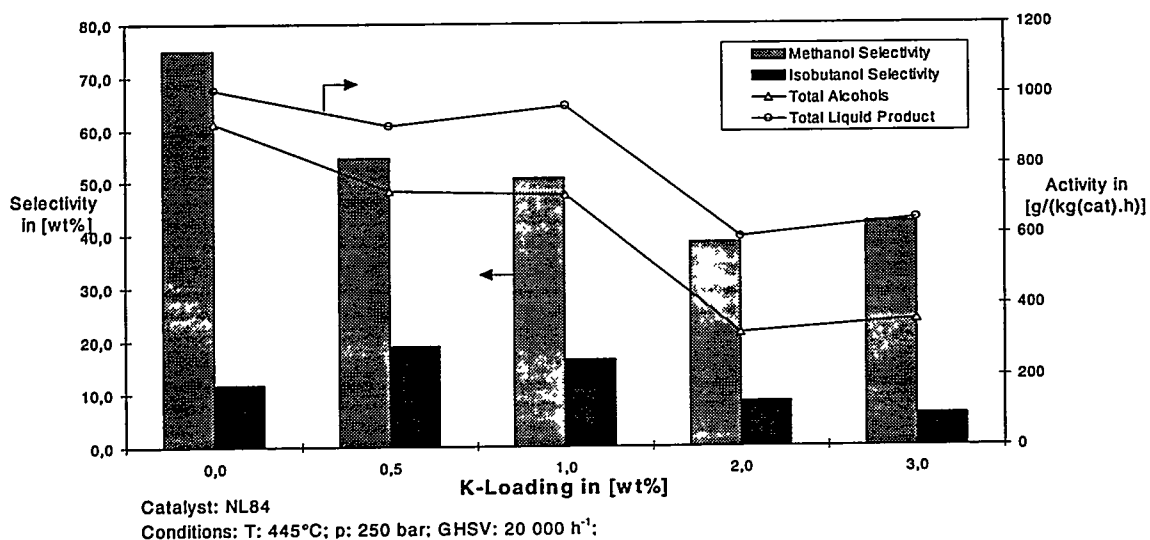
^a GHSV: 20 000 h⁻¹; T: 450°C ; p: 250 bar; CO/H₂: 1:1; particle size: 0.25-0.50 mm.

^b in [g.kg⁻¹ (cat).h⁻¹]

Alkali promotion has been shown to be an important factor in increasing higher alcohol production. Therefore the effect of potassium and cesium on sol-gel catalysts was examined. In contrast to the Cu/Zn oxide system, Table 3.3.2 shows that unpromoted Zr/Zn/Mn oxide catalysts are still able to produce fair amounts of isobutanol. Therefore, the question is whether alkali promotion can bring about a large selectivity shift for these systems as well.

A nitric acid-modified catalyst was chosen for this promoter study, having threshold surface area and pore size distribution values. Promotion was done by impregnation with the necessary amount of alkali acetates, followed by calcination. Catalysis results are displayed in Figures 3.3.1 and 3.3.2.

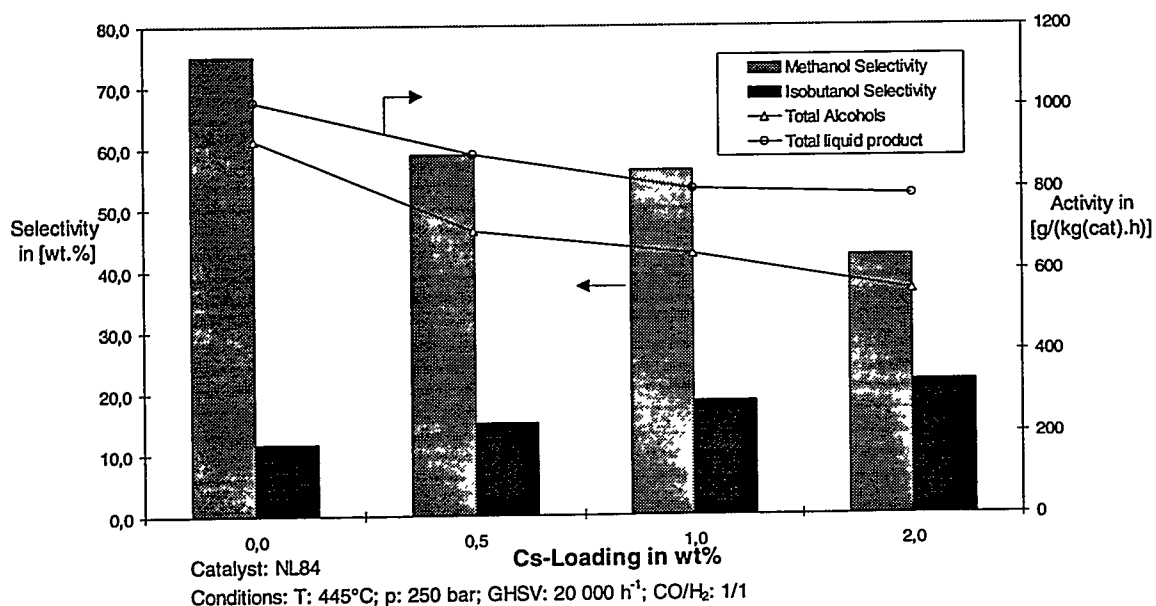
Figure 3.3.1 Influence of Potassium Promotion on Catalyst Behavior



Increasing potassium impregnation leads to a gradual activation decrease. This is probably caused by increased coverage of active sites in combination with a decrease in surface area.

A distinct maximum in isobutanol selectivity and activity is observed at a potassium promotion of 0.5 wt. %.

Figure 3.3.2 Influence of Cesium Promotion on Catalyst Behavior



Cesium promotion shows a different dependence in comparison with potassium promotion. A decrease in activity is also observed, but it is not so drastic as observed for potassium. In contrast, there is no clear maximum in isobutanol selectivity. Increased promotion leads to

higher selectivity for isobutanol. Future work will address this behavior, testing higher cesium loadings and catalyst stability.

Potassium-Promoted ZrO₂/ZnO/Cu₂O Catalysts

Due to the need to develop catalysts that are active at lower temperatures, potassium-promoted ZrO₂/ZnO/Cu₂O catalysts were prepared. These catalysts can easily be synthesized by supercritical extraction from solutions of metal nitrates in solvents with low critical temperatures. The following catalysts were prepared and tested under standard conditions (GHSV = 20000 h⁻¹, p = 25 MPa, T = 400°C, D_{cat} = 0.25-0.50 mm, V_{cat} = 2.5 ml):

BJ 27: Coprecipitated ZrO₂/ZnO/MnO/K- Catalyst sent to Air Products

BJ 45: "Supercritical" ZrO₂/ZnO/MnO- Catalyst with 1.0 wt% K

BJ 47: "Supercritical" ZrO₂/ZnO/Cu₂O- Catalyst with 1.0 wt% K
(Zr:Zn:Cu = 1:3:1)

BJ 49: "Supercritical" ZrO₂/ZnO/Cu₂O- Catalyst with 1.5 wt% K
(Zr:Zn:Cu = 1:3:1)

BJ 50: "Supercritical" ZrO₂/ZnO/Cu₂O- Catalyst with 1.0 wt% K
(Zr:Zn:Cu = 1:1:3)

As shown in Figures 3.3.3 and 3.3.4, the potassium promoted ZrO₂/ZnO/Cu₂O catalysts are higher in selectivity and activity to isobutanol and methanol than the comparable ZrO₂/ZnO/MnO catalysts when run at 400°C.

Figure 3.3.3 Space Time Yields to Isobutanol with Different Catalysts at 400°C

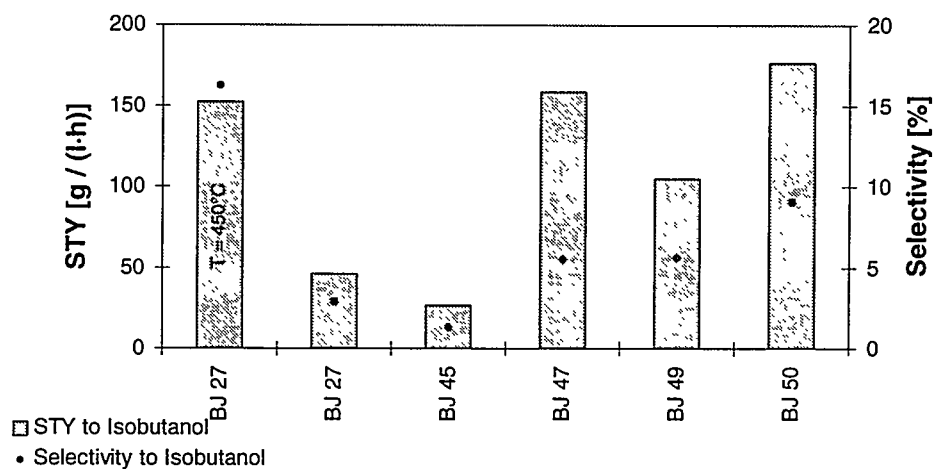
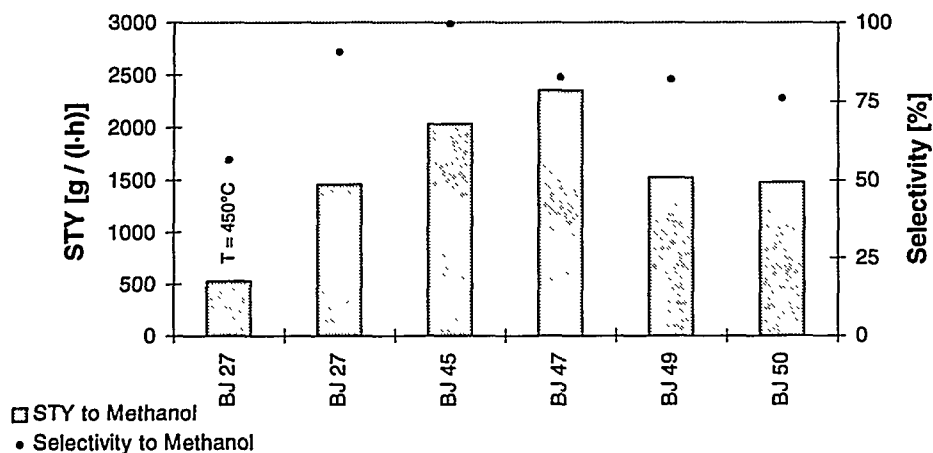


Figure 3.3.4 Space Time Yields to Methanol with Different Catalysts at 400°C



To date, only a first screening could be performed with this new type of catalyst. Further tests with different compositions are under way. The optimized catalyst will then be used for more precise investigations varying temperature, pressure and linear velocity.

Fixed Bed Reactor Runs

A fixed bed reactor study with the potassium-promoted $ZrO_2/ZnO/MnO$ catalyst was performed with different particle sizes and linear velocities. These tests provided data to study the behavior of residence time and temperature on reaction products. Furthermore, mass transfer limitations that affect activity and selectivity can be determined.

For this purpose, after calcination, the catalyst was powdered, pressed and sieved to sizes of 0.25-0.50 mm and 1.60-2.0 mm. Catalyst activations and reactions were carried out in a fixed-bed reactor of stainless steel with an inner diameter of 9 mm. Catalyst particles were mixed with an equal amount of copper particles of the same size. Quartz particles were added on top as a preheating zone.

The catalyst was activated *in situ* by pressurizing with hydrogen (30 $Nl \cdot h^{-1}$, 3 MPa) and heated to 225°C at a rate of 4°/min, keeping this temperature constant for 120 min. Subsequently, the reactor was pressurized with H_2/CO (1/:1) to 25 MPa while temperature was increased to reaction conditions at 4°/min.

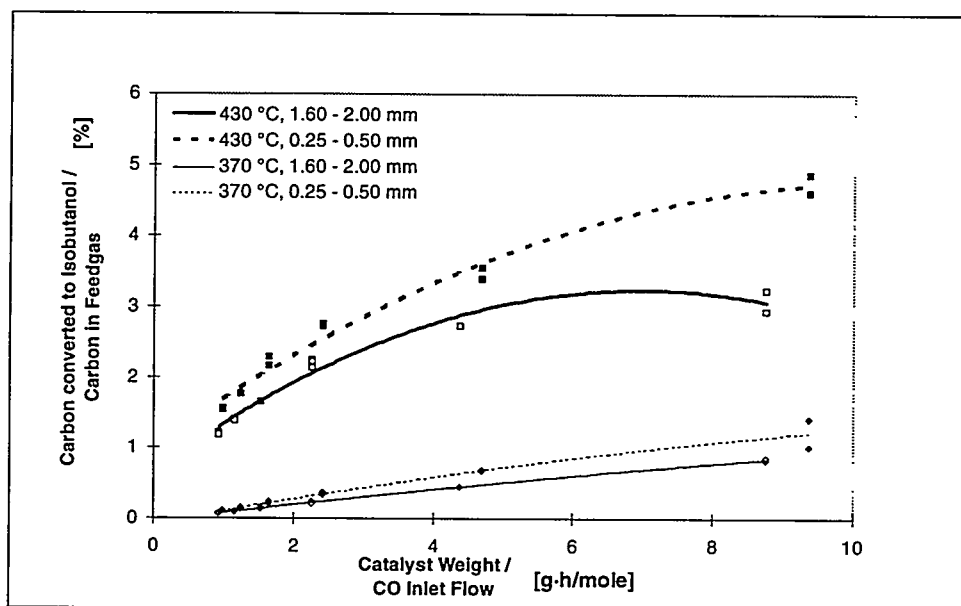
All reactions were conducted at 25 MPa, varying temperature from 430 to 370°C in steps of 30°. Afterwards the measurements at 430°C were repeated to test reproducibility. At each temperature, linear gas velocity was changed in six steps from 24 to 227 $Nl \cdot h^{-1}$. All setpoints were allowed to come to steady state for 75 min. Then the first on-line measurement was started, followed by the collection of one off-line sample. A second on-line measurement 75 minutes later ended each analysis.

With this procedure, four test runs were performed, changing bed volume from 2 to 4 ml of catalyst and particle sizes from 0.25-0.50 to 1.60-2.00 mm.

The fixed-bed reactor study showed that the CO conversion towards alcohols demonstrates a clear dependence upon particle size. All measurements show that activity increases with decreasing particle size, which can be interpreted as mass transfer limitation by pore diffusion.

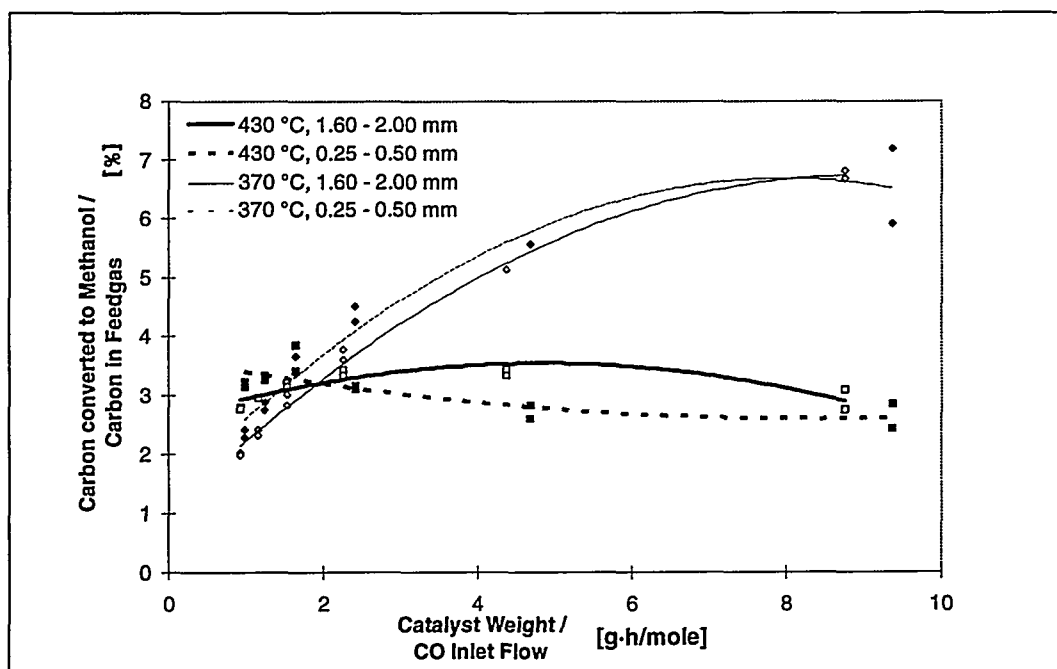
As presented in Figure 3.3.5, CO conversion to isobutanol shows this behavior in a typical way. Activity increases with increasing temperature following Arrhenius' law. The smaller particle sizes show higher conversions than the larger ones, which is an effect of mass transfer limitation. The difference in activity between the two particle sizes grows with temperature due to temperature dependence, which is smaller for mass transfer than for chemical reaction kinetics.

Figure 3.3.5 Effect of Particle Size on CO Conversion to Isobutanol (VCat = 4 ml)



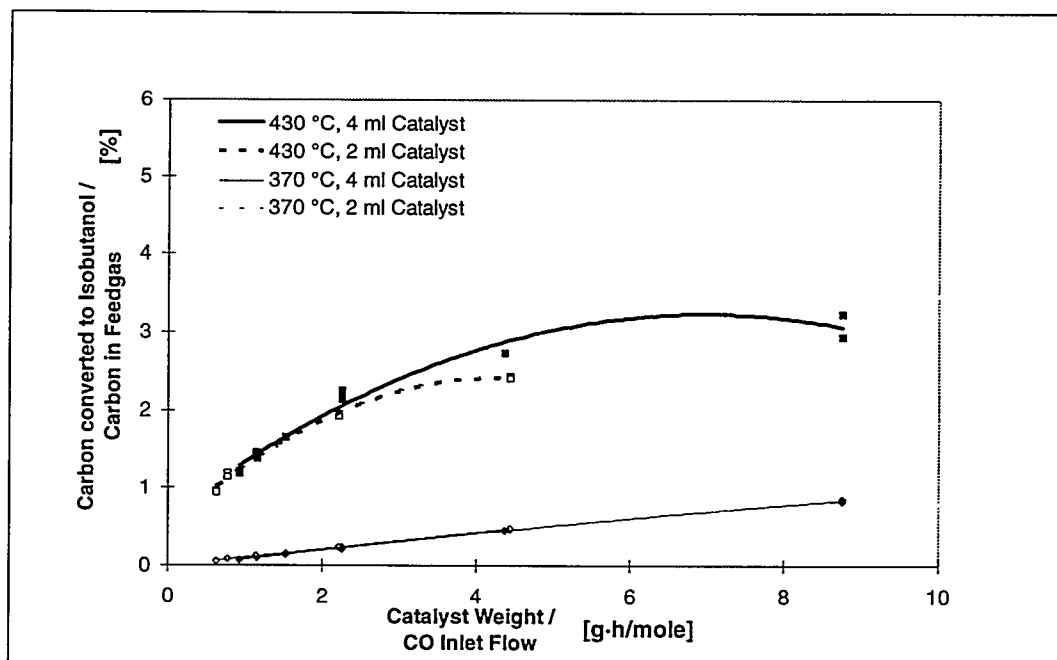
The opposite behavior can be observed for CO conversion to methanol (Figure 3.3.6). The activity decreases with temperature, which can be explained by an approach to chemical equilibrium. At higher temperatures the values are close to equilibrium, and no dependence on residence time can be seen. The measurement at 370°C shows the characteristics discussed above, reaching a steady state value at long residence times in the catalyst bed.

Figure 3.3.6 Effect of Particle Size on CO Conversion to Methanol (VCat = 4 ml)

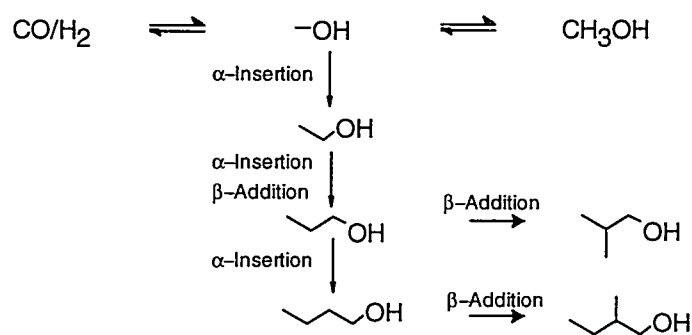


Film diffusion might be an additional limiting step in heterogeneously catalyzed reactions. The influence of film diffusion increases with temperature in the same way as porous diffusion and decreases with linear velocity by reducing laminar films covering the catalyst pellets. Film diffusion was tested for by varying the bed length. Figure 3.3.7 demonstrates that film diffusion has no influence on CO conversion to isobutanol at 370°C and only a little effect at 430°C.

**Figure 3.3.7 Influence of Catalyst Bed Length on CO Conversion to Isobutanol
(Particle Size: 1.60-2.00 mm)**



The most accepted reaction network for higher alcohol synthesis describes the mechanistic differences between the reaction paths to methanol and isobutanol. The first step in higher alcohol synthesis is hydrogenation of CO to a surface intermediate that is very similar to methanol. Linear primary alcohols are built by linear chain growth, including CO insertion steps. Isobutanol and 2-methylbutanol-1 originate from β -addition, including aldolic condensation. Formation of 1-propanol can be reached via both pathways (Scheme 1).

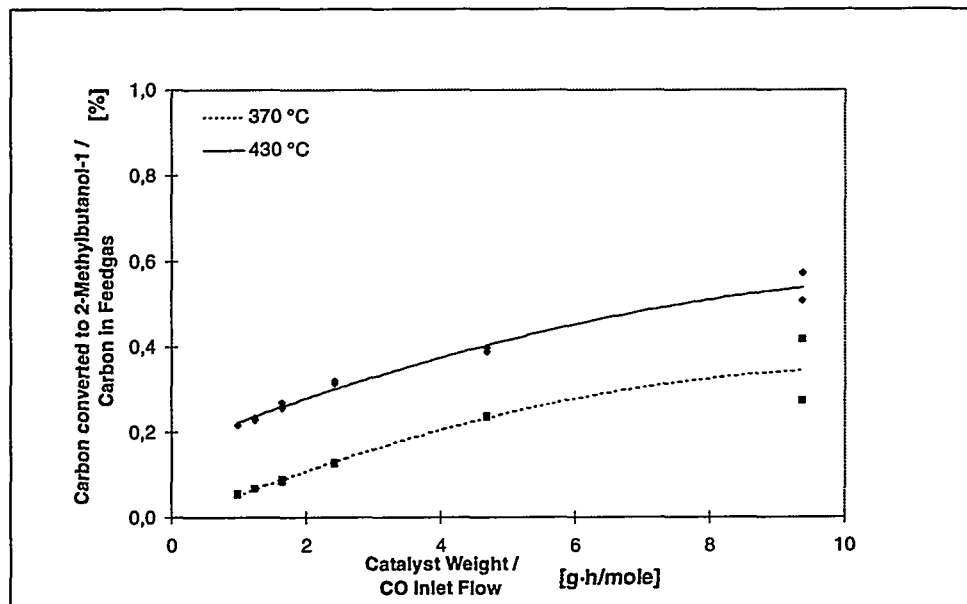


Scheme 1 - Reaction Network for Alcohol Synthesis from CO/H₂

Isobutanol and 2-methylbutanol-1 do not undergo consecutive reactions following this network. They cannot react further in aldolic condensations, and the probability of linear chain growth is low. On the other hand, the linear alcohols are able to undergo linear chain growth as well as β -addition.

The CO conversions to the aforementioned alcohols ethanol, 1-propanol and 2-methylbutanol-1 are plotted in Figures 3.3.8, 3.3.9 and 3.3.10, respectively. The branched alcohol 2-methylbutanol-1 shows similarities to the conversion to isobutanol, with an increasing activity with temperature (Figure 3.3.8).

Figure 3.3.8 CO Conversion to 2-Methylbutanol-1 (VCat = 4 ml, Particle Size: 0.25-0.50 mm)



The conversions to ethanol (Figure 3.3.9) and 1-propanol (Figure 3.3.10) show behavior similar to that described for methanol. They exhibit a lower activity at higher temperature and seem to be independent of linear gas velocity at 430°C.

Figure 3.3.9 CO Conversion to Ethanol (VCat = 4 ml, Particle Size: 0.25-0.50 mm)

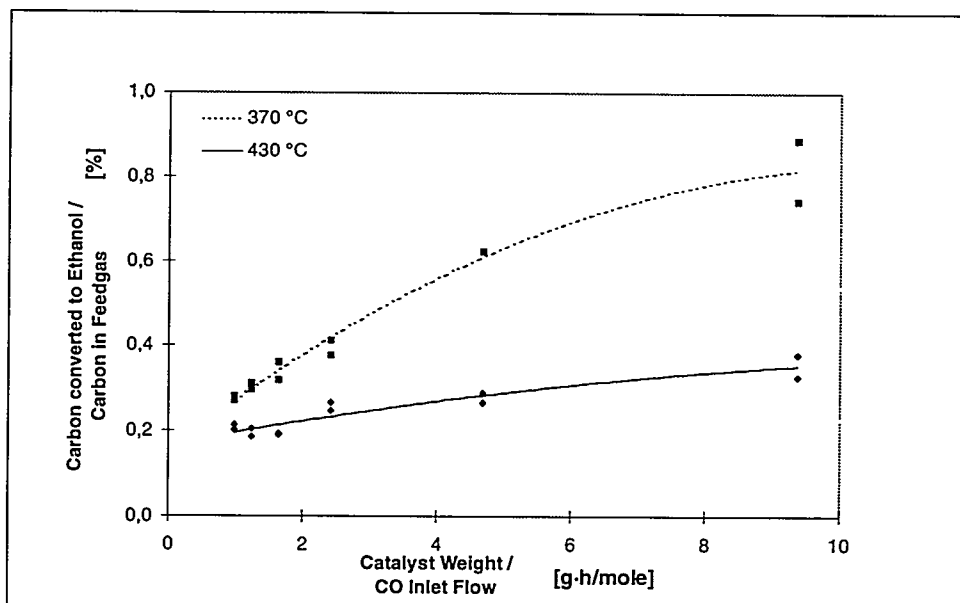
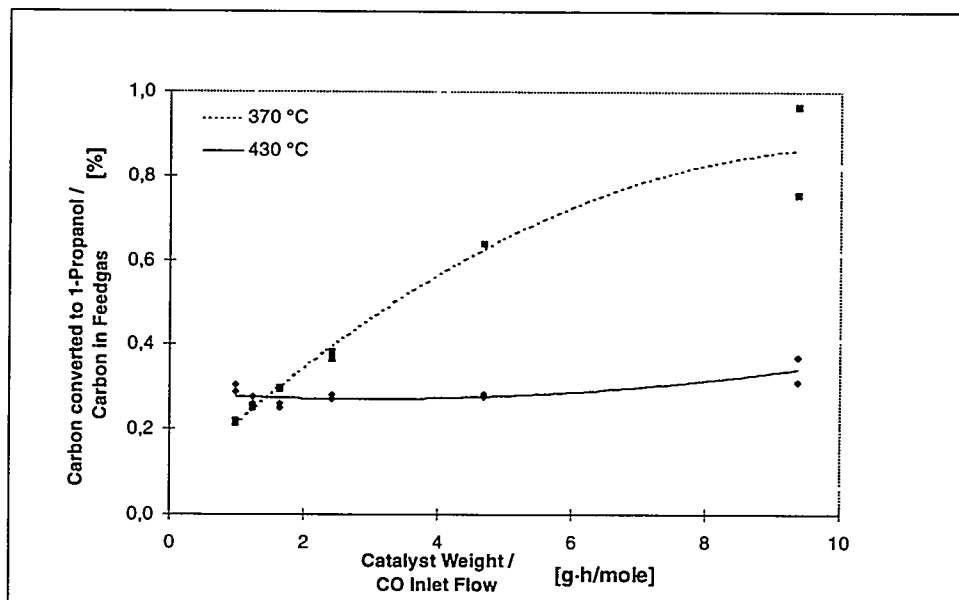


Figure 3.3.10 CO Conversion to 1-Propanol (VCat = 4 ml, Particle Size: 0.25-0.50 mm)



Slurry Reactor Design and Runs

In the last quarter, work dealt with mass transfer and the influence of pressure. Mass transfer was examined in the three-phase system, and the influence of reaction pressure on the yield was tested in two- and three-phase systems.

Mass Transfer

Tests studying the mass transfer in a slurry reactor under isobutanol synthesis conditions were performed. Under such conditions, no mass transfer limitation could be proven. This result agrees with former theoretical conclusions (see quarterly report for Oct.-Dec. 1995). The maximum amount of catalyst suspended in decalin was 25 wt%.

The procedure for these tests was as follows. Six runs were executed, including reduction and reaction. Between two runs, catalyst loading was increased and suspension level in the reactor was checked (Table 3.3.3). This procedure was followed by the three steps listed in Table 3.3.4, which were performed with the GHSV at a constant level. The reaction temperature was kept constant at 400°C. All measurements listed below were carried out during step three.

Table 3.3.3 Catalyst Content in Slurry Runs Testing Mass Transfer

Run	1	2	3	4	5	6
Catalyst volume ^a [ml]	6	11.9	17.9	23.9	29.9	32.8
Catalyst weight [g]	8	16	24	32	40	44
Catalyst ratio [wt%]	5.8	11	15.7	19.9	13.7	25.4

^a corresponding to the catalyst volume of the fixed-bed reactor

Table 3.3.4 Reaction Conditions in Slurry Runs Testing Mass Transfer

Step	Conditions
I reduction	gas H ₂ pressure = 3 MPa mass flow = 30 NI/h temperature = 225°C for 120 min
II reaction	feedstock CO/H ₂ pressure = 25 MPa mass flow = 115 NI/h over night temperature = 400 °C
III reaction	feedstock CO/H ₂ pressure = 25 MPa GHSV = 8700 h ⁻¹ temperature = 400°C
constant:	catalyst ZnO/Cr ₂ O ₃ /K ₂ O (BASF) particle size 63-160 μm heating rate 4°C/min temperature of the preheater 385°C temperature of the reflux condenser 160°C slurry volume 150 cc stirrer speed 2500 rpm

Each measurement was repeated three times. The results of the different runs were linked by a polynomial regression of the 2nd order.

As mentioned above, mass transfer limitation has to be excluded (Figure 3.3.11). The mass of CO converted per unit of time increases slightly more than linearly. The identical effect is shown in Figure 3.3.12. CO conversion is not absolutely equal over the whole range, but increases from

to 25%. An explanation could be the diminution of surface effects at higher catalyst loadings; the relative amount of catalyst hidden at the reactor walls, at the housing of the stirrer head and in tubing system becomes smaller. This possibility also explains the increase in STY towards isobutanol and methanol. Concurrently the selectivity to CO₂ decreases. A further explanation of the decrease in selectivity to CO₂ could be given by the shortened residence time at higher catalyst loadings.

Figure 3.3.11 Converted CO vs Catalyst Volume Testing Mass Transfer

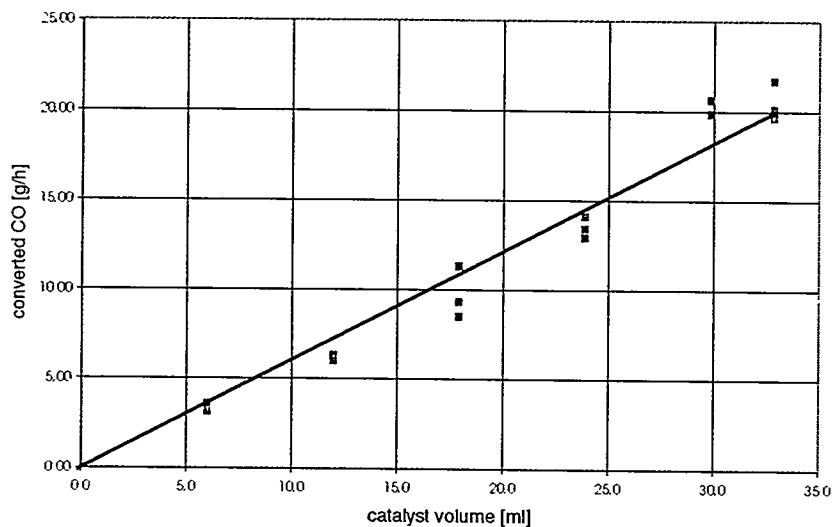
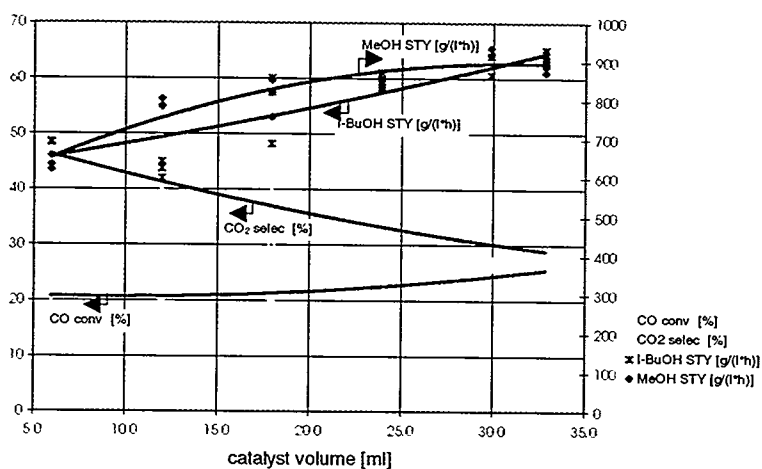


Figure 3.3.12 Yields by Runs Testing Mass Transfer Given in Relative Quantities



The results mentioned above were confirmed by experiments using the CSTR without decalin as a two-phase system. With similar residence time and gas hourly space velocity, the yield from a two- and a three- phase system is comparable (each CSTR). This gives a further hint that isobutanol synthesis under the reaction conditions mentioned above is limited by its intrinsic reaction rate.

Influence of Pressure

An increase in reaction pressure causes a rise in the residence time and an increase in concentration in the gas phase. It is not possible to distinguish between the influence of residence time and concentration as long as a kinetic rate expression is not available.

However, the relative increase in yield is higher as the relative increase in reaction pressure. This was experimentally shown in the pressure range from 17 MPa up to 33 MPa. The experiments were made using the fixed-bed reactor as well as the CSTR. The increase in yield to isobutanol depends on reaction temperature and reactor type (Figures 3.3.13-3.3.15). The yield to methanol rises to the new value of the thermodynamic equilibrium (Figures 3.3.16-3.3.18). The relative increase in methanol is therefore similar for both reactors. Ignoring the results from three-phase CSTR runs, which have a higher systematic error in measurement, the STY towards methanol increases by a factor in the range of 2.4 up to 2.8, while the pressure is nearly doubled from 17 MPa up to 33 MPa (Table 3.3.5). The same pressure rise causes an increase in STY towards isobutanol by a factor in the range of 2.0 to 3.3. Remarkable is the contrasting behavior of the fixed bed reactor and the two-phase CSTR. The relative amount of isobutanol made in the fixed-bed reactor increases with decreasing temperature. The formation of by-products in the fixed-bed reactor seems to be so strong at high temperatures that the advantage obtained by an increase in concentration and residence time is not realized entirely anymore.

The shape of the curves for the CSTR as two- or three- phase system is similar.

Table 3.3.5 Relative Increase in Isobutanol and Methanol by Increasing Pressure from 17 up to 33 MPa for Various Temperatures and Reactors (ZnO/Cr₂O₃/K-Catalyst)

reaction conditions reactor	isobutanol			methanol		
	fixed bed	two phase CSTR	three phase CSTR	fixed bed	two phase CSTR	three phase CSTR
GHSV [h ⁻¹] corresponding to Figure	23000 3	9500 4	19000 5	23000 6	9500 7	19000 8
385°C	3.3	2.0	2.3	2.5	2.6	2.0
400°C	2.8	2.3	2.3	2.4	2.6	2.5
415°C	2.4	2.5	2.1	2.5	2.8	3.1

Figure 3.3.13 STY Isobutanol vs Reaction Pressure (Fixed-Bed Reactor, ZnO/Cr2O3/K-Catalyst, V_{cat} = 5 ml, GHSV = 23000 h⁻¹)

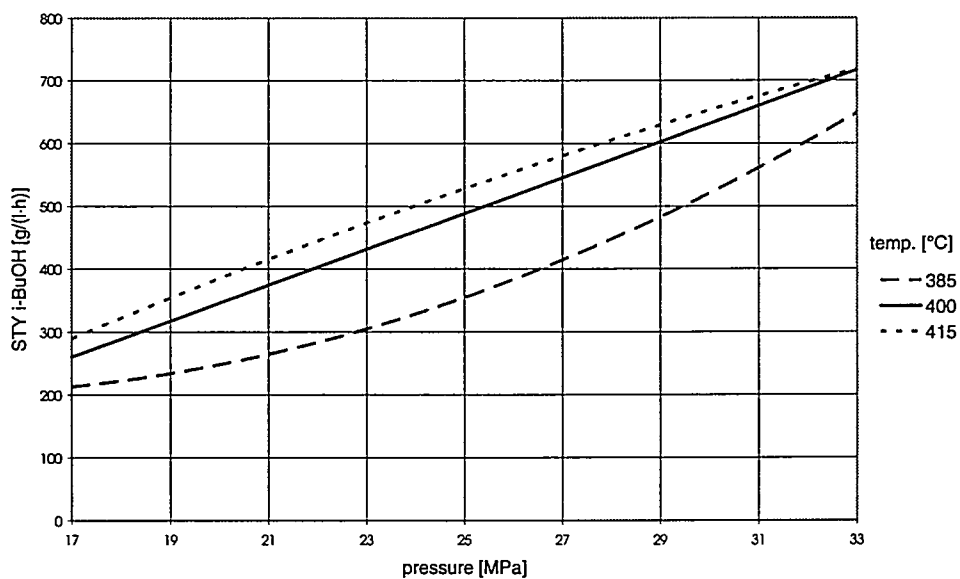


Figure 3.3.14 STY Isobutanol vs Reaction Pressure (Two-Phase CSTR, ZnO/Cr2O3/K-Catalyst, V_{cat} = 17.9 ml, GHSV = 9500 h⁻¹)

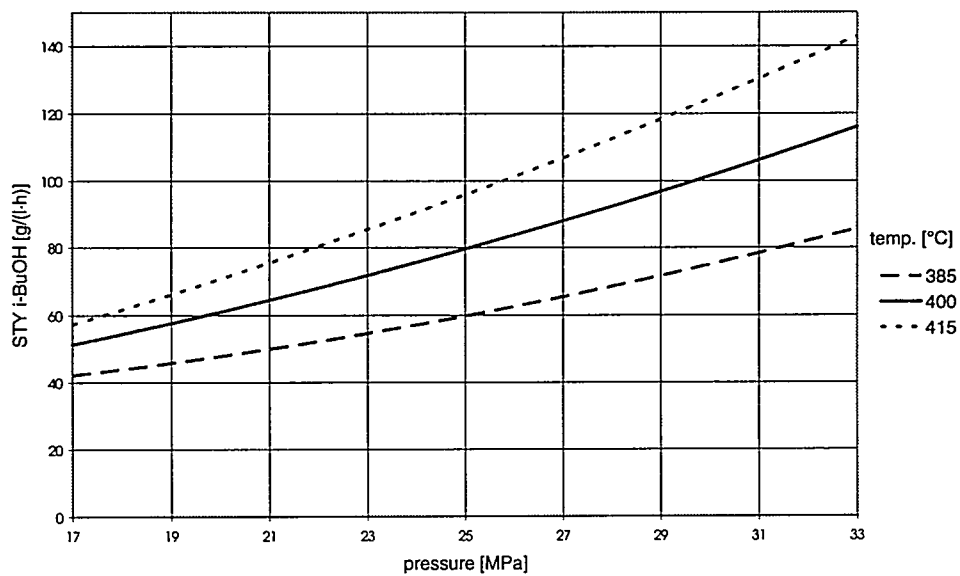


Figure 3.3.15 STY Isobutanol vs Reaction Pressure (Three-Phase CSTR, ZnO/Cr2O3/K-Catalyst, V_{cat} = 6 ml, GHSV = 19000 h⁻¹)

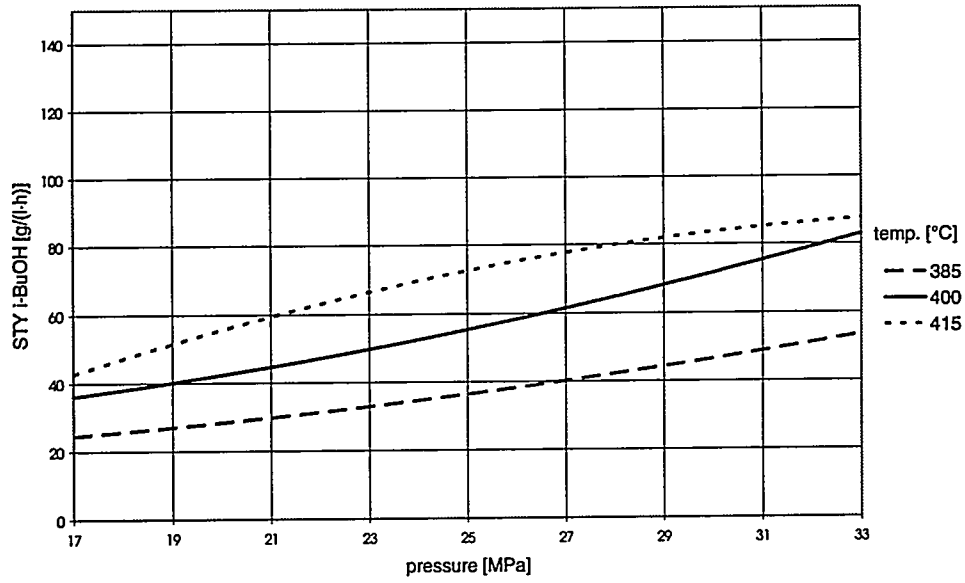


Figure 3.3.16 STY Methanol vs Reaction Pressure (Fixed-Bed Reactor, ZnO/Cr2O3/K-Catalyst, V_{cat} = 5 ml, GHSV = 23000 h⁻¹)

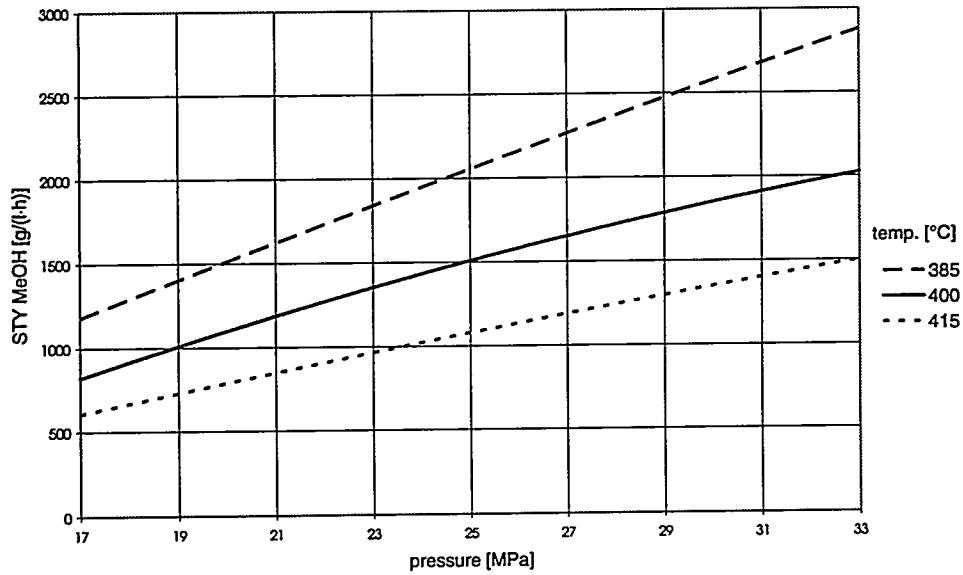


Figure 3.3.17 STY Methanol vs Reaction Pressure (Two-Phase CSTR, ZnO/Cr2O3/K-Catalyst, V_{cat} = 17.9 ml, GHSV = 9500 h⁻¹)

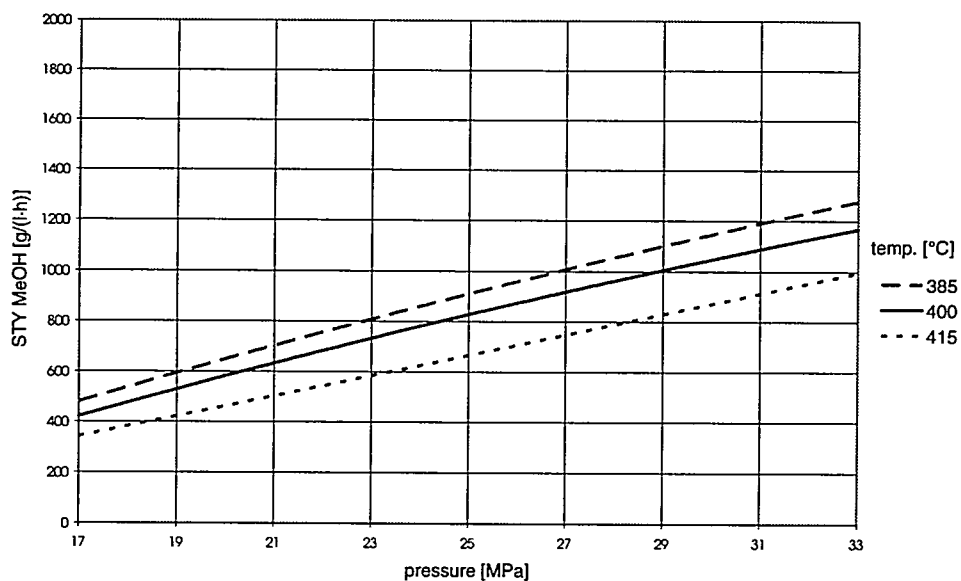


Figure 3.3.18 STY Methanol vs Reaction Pressure (Three-Phase CSTR, ZnO/Cr2O3/K-Catalyst, V_{cat} = 6 ml, GHSV = 19000 h⁻¹)

